Applied Geochemistry 96 (2018) 24–34

Contents lists available at ScienceDirect

Applied Geochemistry

journal homepage: www.elsevier.com/locate/apgeochem

Ge/Si ratios point to increased contribution from deeper mineral weathering to streams after forest conversion to cropland

Yolanda Ameijeiras-Mariño[a], Sophie Opfergelt[a,*], Louis A. Derry[b], Jérémy Robinet[c], Gerard Govers[c], Jean P.G. Minella[d], Pierre Delmelle[a]

[a] Earth and Life Institute, Environmental Sciences, Université catholique de Louvain, L7.05.10, 1348, Louvain-la-Neuve, Belgium
[b] Department of Earth and Atmospheric Sciences, Cornell University, Ithaca, NY, 14853, USA
[c] Department of Earth and Environmental Sciences, KU Leuven, Celestijnenlaan 200 E, 3001, Leuven, Belgium
[d] Department of Soils, Federal University of Santa Maria, 97105-900, Santa Maria, Brazil

ARTICLE INFO

Editorial handling by Neus Otero

Keywords:
Ge/Si ratio
Mineral weathering
Forest conversion
Brazil

ABSTRACT

The impact of forest conversion on soil weathering is studied in a subtropical humid setting in southern Brazil (Rio Grande do Sul). A geochemical tracer of mineral weathering processes, the Ge/Si ratio, was used at the pedon and catchment scales to compare a cropland and a forest catchment. Ge/Si measurements were performed on bedrock, bulk soil, soil pore water and stream waters during base flow and rain events. The Ge/Si ratio in bulk soils is interpreted as the result of a mixing between clay minerals and quartz. Based on the Ge/Si ratio in soil pore water, no change in mineral weathering has been induced by forest conversion at the pedon scale. In contrast, at the catchment scale, the Ge/Si ratio of stream waters indicates an increased contribution from mineral weathering after conversion of forest to cropland. The evolution of Ge/Si ratio in stream waters during rain events points to a change in the hydrological paths due to forest conversion. We argue that forest conversion to cropland led to increased water percolation in soil, allowing the weathering of deeper soil material and thus, a stronger contribution from mineral weathering to stream waters.

1. Introduction

Vegetation type, soil water availability and erosion rates are key factors that govern the chemical weathering of minerals (e.g., Drever, 1994; Millot et al., 2002; Dixon et al., 2009). Growing world population places a high demand for arable lands, resulting in increased conversion of forests to croplands (Godfray et al., 2010; Foley, 2011). Such land use changes impact on vegetation cover, soil hydrology and soil erosion (e.g., Costa et al., 2003; Brown et al., 2005; Pimentel, 2006; Quinton et al., 2010; Molina et al., 2012), which in turn may influence chemical weathering processes in soil (e.g., Lucas, 2001; Maher, 2010).

The presence of plants alters the soil weathering conditions, mainly by changes in pH and in the concentration in dissolved elements in soil pore water (e.g., Lucas, 2001). Forest conversion to cropland alters plant element uptake, litter fall decay, and hence, the element cycling of the forested ecosystems (e.g., Lucas et al., 1993; Alexandre et al., 1997; Lucas, 2001). As shown for Si in the context of deforestation, the dissolved element fluxes at the catchment scale increase immediately after deforestation (Conley et al., 2008) but decrease in the long term (Struyf et al., 2010; Carey and Fulweiler, 2012). These studies mainly attribute the observed changes in dissolved Si fluxes to changes in the biogenic silicon pool (phytoliths) in soils, but the contribution from mineral weathering to dissolved Si fluxes has not been specifically considered.

Conversion of forest to cropland also modifies soil hydrology and hence, critically, the amount of water available for weathering reactions (e.g., Dixon et al., 2009; Maher, 2010; Rasmussen et al., 2011; Ferrier et al., 2012). This is due (i) to less evapotranspiration taking place in croplands than in forests (e.g., Foley et al., 2005) and (ii) to destruction of the macropore-driven lateral water pathways which result from roots and biological activity and which normally prevail in forested ecosystems (Uchida et al., 2001; Bachmair and Weiler, 2011; Beven and Germann, 2013). Further, soil tillage in croplands typically accelerates erosion compared to forests (Meade et al., 1990; Pimentel, 2006; Montgomery, 2007). This may expose deeper soil layers containing less weathered mineral surfaces to chemical weathering (Millot et al., 2002).

Changes in mineral weathering following conversion of forest to

* Corresponding author.
E-mail addresses: yolanda.ameijeiras@uclouvain.be (Y. Ameijeiras-Mariño), sophie.opfergelt@uclouvain.be (S. Opfergelt), derry@cornell.edu (L.A. Derry), jeremy.robinet@kuleuven.be (J. Robinet), gerard.govers@kuleuven.be (G. Govers), jminella@smail.ufsm.br (J.P.G. Minella), pierre.delmelle@uclouvain.be (P. Delmelle).

https://doi.org/10.1016/j.apgeochem.2018.06.002
Received 22 November 2017; Received in revised form 29 May 2018; Accepted 6 June 2018

cropland remain largely unexplored despite important implications for the global biogeochemical cycles of key elements, such as C and Si (Struyf et al., 2010; Goudie and Viles, 2012). Changes in the mineral weathering contribution to element fluxes are often investigated at the catchment scales by monitoring the concentrations of Si and major cations in river waters (e.g., Gaillardet et al., 1999; Jacobson et al., 2003; Moon et al., 2014). Conversion of a forest to a cropland modifies the Si biogeochemical cycle in the soil-plant system (Struyf et al., 2010; Carey and Fulweiler, 2012) and thereby, the relative contributions of biogenic and non-biogenic sources and processes to dissolved Si in rivers. This jeopardizes the use of riverine Si concentrations to assess the impact of land use change on weathering. However, monitoring of the Ge/Si ratio may help to circumvent this issue. Since Ge substitutes for Si during clay formation, soils are generally characterised by higher Ge/Si ratios than their parent materials (Murnane and Stallard, 1990; Kurtz et al., 2002). Conversely, soil pore water and streams display lower Ge/Si values than the bedrock (Mortlock and Froelich, 1987). Due to discrimination against Ge by plants, phytoliths display among the lowest Ge/Si ratios (Derry et al., 2005; Blecker et al., 2007). Thus, Ge/Si ratio has been used as a geochemical tracer to study silicate weathering (e.g., Mortlock and Froelich, 1987; Murnane and Stallard, 1990; Froelich et al., 1992; Kurtz et al., 2002) and the biological cycle of Si (Derry et al., 2005; Cornélis et al., 2011).

Here, we report the results of a study aimed at assessing the impact of forest conversion to cropland on mineral weathering in a subtropical humid region in southern Brazil. To do this, we measured the Ge/Si ratio in a variety of soil and water samples from a forested and a cropland catchment.

2. Environmental setting

The study area is located in the southernmost state of Brazil, Rio Grande do Sul, situated on the Rio-Grandense plateau (Fig. 1). Agricultural development started around 1925 and was gradually intensified until reaching a peak in the early 1960s (Lopes, 2006; Minella et al., 2008). The climate is subtropical super-humid mesothermic (Köppen classification; Minella et al., 2008). The mean annual temperature and rainfall fluctuate between 14 and 18 °C and between 1700 and 1800 mm, respectively (Minella et al., 2014). The soils belong to the Acrisols, Cambisols and Leptosols types (IUSS Working Group WRB, 2007). Topography is characterised by slopes between 4 and 84° (Minella, 2003). At the altitude of the study site (650–730 m above sea level), the parent material is rhyodacitic and the mineralogy is dominated by quartz (~38%) and sanidine (K-feldspar; ~45–55%). Hematite and goethite occur in minor amounts. A basaltic lithology dominates at lower altitudes (Bellieni et al., 1986; Montanheiro et al., 2004).

A native semi-deciduous forest catchment was selected as the natural reference (near Ilópolis, 28°56′1.03″S - 52° 6′28.44″W, surface area of 0.03 km^2; Fig. 1a). *Araucaria angustifolia*, *Luehea divaricata*, *Nectandra Grandiflora* and *Campomanesia guaviroba* are the most representative species. The cropland catchment (Arvorezinha; 28°49′55.90″S - 52°13′12.12″W) is located 20 km from the forested catchment (Fig. 1a) and has a surface area of 1.19 km^2. A smaller sub-catchment (0.14 km^2, five times larger than the forest catchment) was also defined within the cropland catchment (Fig. 1b) to be more comparable to the size of the forest catchment than the whole cropland catchment (40 times larger than the forest catchment). Information on land use in the cropland catchment for the past 50 years and sediment export between 2002 and 2011 is available from Minella et al. (2014). The main crops are tobacco (*Nicotiana tabacum*), maize (*Zea mays)* and soybean (*Glycine max*). These are cultivated with a frequency dictated by market prices. Black oat is sometimes used as a cover crop. The soil is prepared for seeding between August and September, and the scarce vegetation residues from the precedent harvest are ploughed back into the soil. Seeding begins in September–October and consequently, the soil cover is minimal at the time of the year characterised by the highest rainfall erosivity (September; Ramon et al., 2017). Harvest takes place between January and February. Between March and August, some fields remain abandoned, with spontaneous winter vegetation, whereas others are planted with a winter vegetation cover.

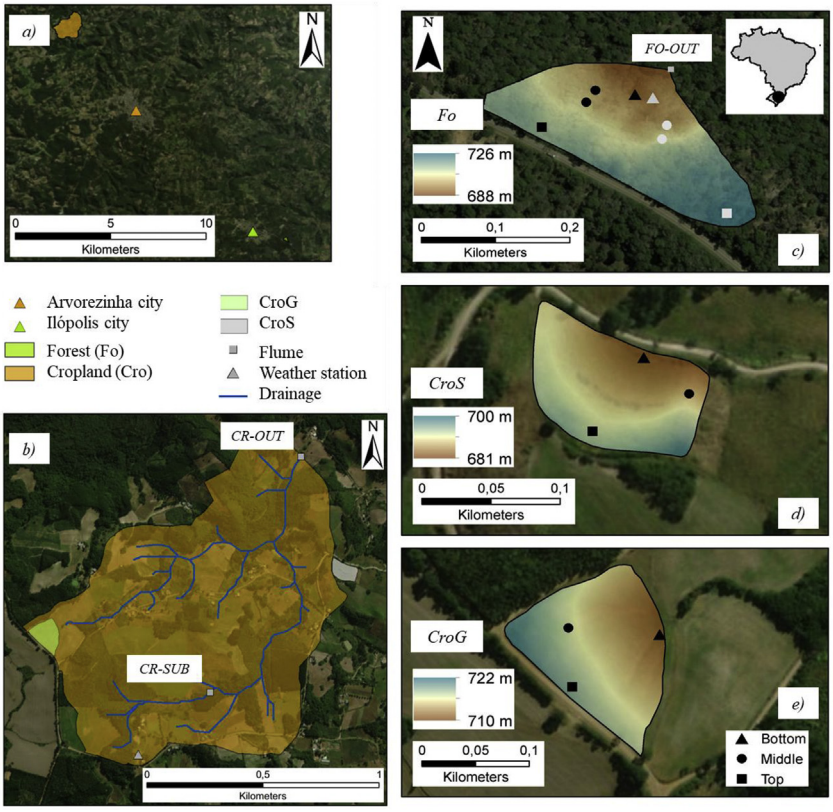

Fig. 1. Location of the study site in Brazil (upper right box). a) Location of Arvorezinha and Ilópolis cities and the cropland (Cro) and forest (Fo) study areas (note that the forest study area is a small green area East of Ilópolis city). b) Relative position of the two cropland slopes within the cropland study area (CroS = steep in grey; CroG = gentle in green) and position of the flumes for river sampling (grey squares labelled CR-OUT and CR-SUB). c) Position along the slope of the sampled soil profiles in the forest slopes: steep (FoS, white symbols) and gentle (FoG, black symbols); position of the flume for river sampling (small grey square at the bottom of the slope labelled FO-OUT). d) Position along the slope of the sampled soil profiles in the cropland steep slope (CroS). e) Position along the slope of the sampled soil profiles in the cropland gentle slope (CroG). (For interpretation of the references to colour in this figure legend, the reader is referred to the web version of this article.)

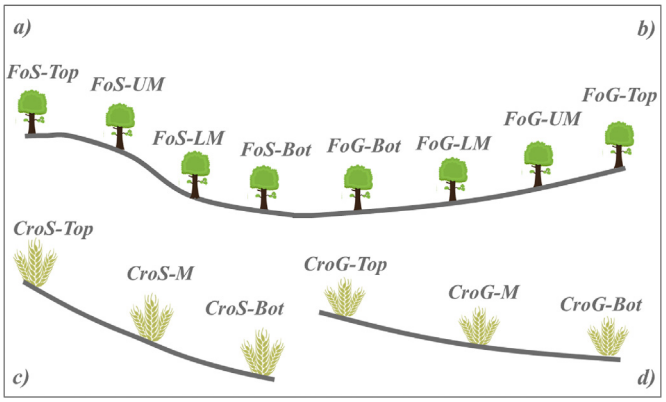

Fig. 2. Schematic representing the three sample positions, i.e. top, middle and bottom, along the slopes. a) forest steep slope (FoS); b) forest gentle slope (FoG); c) cropland steep slope (CroS); d) cropland gentle slope (CroG). Top: top, UM: upper middle, LM: lower middle, Bot: bottom.

3. Methods

3.1. Sampling

3.1.1. Bulk soils and bedrock samples

Bedrock and soil samples were collected in July–August 2014. Bedrock fragments were sampled from outcrops in each catchment. Two different slopes were selected in both the forest (Fo) and cropland (Cro) sites (Fig. 1c, d and e) in order to account for conditions less favourable to erosion in gentle slope (G; average on the middle of the slope: 9 ± 2°) and more favourable to erosion in steep slope (S; average on the middle of the slope: 15 ± 3°). On each slope, different soil positions were sampled to cover the eroding zone at the summit (top position Top), the intermediate zone in the middle position (M; with two middle positions in the forest catchment defined as Upper Middle, UM, and Lower Middle, LM), and the bottom of the slope (bottom, Bot). The bottom position was considered as the deposition zone accumulating eroding material from upslope (Fig. 2). The soil was sampled at two depths (20–30 cm and 55–65 cm) to investigate the evolution of the Ge/Si ratio within the soil profile. The full characterization of the soil and bedrock samples is provided elsewhere (Ameijeiras-Mariño et al., Schoonejans et al., 2017) and the key soil properties are presented in Table A1.

3.1.2. Soil pore water

Soil pore water was collected at the forest and cropland sites every week during five weeks between October 7th and November 8th, 2014. In cropland, soil pore water was collected at the beginning of the seeding season, i.e. tobacco in steep slope and soybean in gentle slope. Suction cups with a porous membrane of 0.45 µm pore size (Eijkelkamp®) were installed at 70 cm depth at all slope positions, except for the forest steep upper middle (FoS-UM) where the soil was shallower than 50 cm. The cups were installed one month before sampling. Vacuum was applied with a hand pump to initiate water sampling. The soil pore water was not collected during the first month to allow soil recovery from the disturbance induced during installation. Then, soil pore water samples were collected during five weeks (once per week) in pre-cleaned polypropylene copolymer (PPCO) bottles and acidified with 1% HNO_3 (suprapur).

3.1.3. Stream waters

Stream water samples were collected between October 12th and November 5th, 2014 at the outlet of the forest and cropland catchments (Fig. 1b and c). The streams sampled include water from the whole forest catchment outlet (FO-OUT; 0.03 km^2), the whole cropland catchment outlet (CR-OUT; 1.19 km^2), and the smaller sub-catchment within the cropland catchment (CR-SUB; 0.14 km^2, to compare with the smaller surface area of the forested catchment). Stream water samples at the three sampling points were collected during base flow and during rain events (at fixed water level increments). Samples were collected in plastic bottles connected to an automatic sampling device (ISCO system), and filtered within 24 h using polycarbonate filters (0.45 µm pore size). After filtration, the samples were collected in PPCO bottles previously cleaned with 2.5% HNO_3 (commercial) and acidified to 1% HNO_3 (suprapur).

Stream water samples were sampled at base flow, three times in forest at FO-OUT between 22nd October and 4th November 2014, and four times in cropland at both CR-SUB and CR-OUT between 21st October and 5th November 2014. Stream water samples were also collected during rain events in forest and cropland. The sampling covers rain events with lower and higher change in stream water discharge and were monitored during deviation (rising limb) and return to base flow levels (falling limb). Under forest, stream waters were sampled during: (i) a small rain event with an increase of ~ three times of the stream discharge (from between 1 and 21 $l\,s^{-1}\,km^{-2}$ during base flow up to 56 and 58 $L\,s^{-1}\,km^{-2}$ during the rain event, standardised to the catchment size) on 12th October 2014 during 1 h (n = 6). The sampling started when the discharge was already higher than the base flow level; (ii) a large rain event of ~24 h with an increase of ~40 times of the discharge (discharge variation between 96 and 839 $L\,s^{-1}\,km^{-2}$ during the event, as compared to between 1 and 21 $L\,s^{-1}\,km^{-2}$ during base flow) on 16–17th October 2014 (n = 21). The sampling stopped before the return to base flow level. Under cropland, stream waters were sampled during one rain event on 13–14th October 2014: (i) at the outlet of the whole catchment (n = 4, covering a portion of the rain event) where the discharge increased ~ 12 times (from base flow discharge of 16–20 $L\,s^{-1}\,km^{-2}$ to a range between 65 and 242 $L\,s^{-1}\,km^{-2}$ during the event); and (ii) at the sub-catchment (n = 10, covering nearly the entire rain event) where the discharge increased ~ 38 times (from 8 to 11 $L\,s^{-1}\,km^{-2}$ during base flow level to a range between 34 and 420 $L\,s^{-1}\,km^{-2}$ during the rain event).

3.2. Si and Ge measurements

The bedrock and soil (fraction < 2 mm) samples were crushed within an agate mortar prior to analysis. The soil and bedrock materials were dissolved by lithium metaborate and tetraborate fusion (Chao and Sanzolone, 1992). The Si concentration of the bedrock, soil, soil pore water and stream water samples was measured by ICP-AES (1.3% uncertainty relative to standard material). Major elements concentrations in soil pore water and river waters are provided in the Appendix (Tables A2 and A3 respectively).

Germanium measurements in the soil, bedrock, soil pore water and stream waters were performed by high resolution inductively coupled plasma mass spectrometer (HR-ICP-MS, Element2, Thermo Fischer Scientific, Department of Earth and Atmospheric Sciences of Cornell University, Ithaca, NY) using a hydride generation system and applying the isotope dilution technique (Mortlock and Froelich, 1996). Soil and bedrock samples were first dissolved by microwave digestion of the finely crushed powder at 220 °C with HNO_3-HCl-HF. After cooling to room temperature, the digestion vessel was opened and H_3BO_3 was added. The vessel was sealed and re-heated to 120 °C in order to prevent volatilisation of Ge and Si fluoride compounds. After cooling down to room temperature, the solution was diluted with ultrapure water and heated at 50 °C during one night to prevent silica precipitation. A spike enriched in ^{70}Ge was added to liquid samples (either water or digested soil or bedrock) at least 24 h prior to analysis, the samples were well mixed with the spike and left for equilibration at ~80 °C overnight. The target $^{70}Ge/^{74}Ge$ ratio of spiked samples was ca. 5–15, relative to a natural ratio of 0.5635 (Kipphardt et al., 1999). After equilibration of the spike, the sample was fed to an online hydride generation system with $NaBH_4$ and HNO_3 to produce the germane species. The reacting

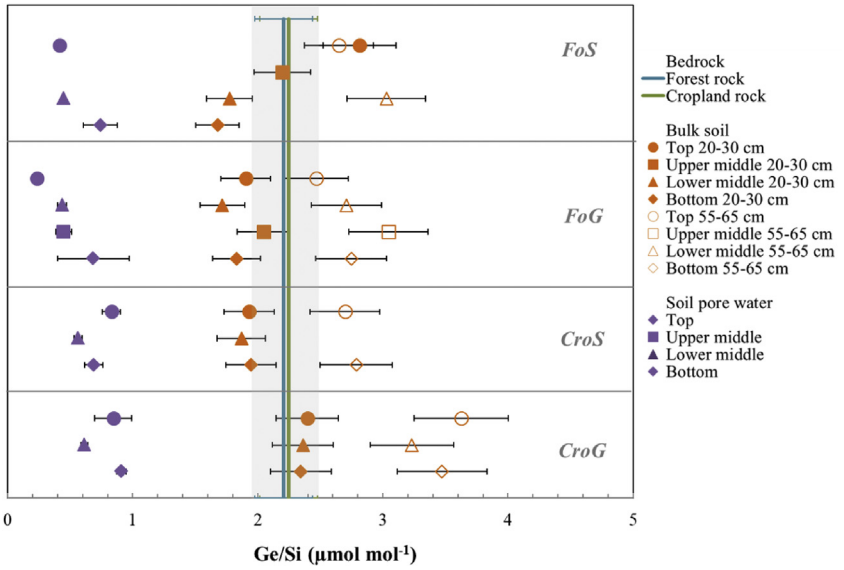

Fig. 3. Ge/Si ratios (± SD) of the soil at two depths (20–30 cm and 55–65 cm; orange symbols) and soil pore water (at 70 cm; purple symbols) samples grouped by slope and slope position (average for five weeks ± SD). FoS: forest steep slope; FoG: forest gentle slope; CroS: cropland steep slope; CroG: cropland gentle slope. The vertical lines represent the Ge/Si ratio of the bedrock from each catchment. (For interpretation of the references to colour in this figure legend, the reader is referred to the web version of this article.)

solution was sparged with Ar and the volatile Ge passed through a PTFE membrane gas-liquid separator and directly into the torch of the ICP-MS. $^{70}Ge/^{74}Ge$ ratios were measured using the low mass resolution slit settings in ion counting mode. Mass bias was corrected from analysis of unspiked standards, yielding in a typical precision on $^{70}Ge/^{74}Ge$ of ± 2% RSD (e.g., Derry et al., 2005; Lugolobi et al., 2010; Kurtz et al., 2011).

4. Results

The Ge/Si ratios of the bedrock, bulk soil, soil pore water and stream water samples are shown in Fig. 3 (bedrock, bulk soil and soil pore water), Fig. 4 (soil pore water and stream water base flow), Fig. 5 (stream waters during rain events), Table 1 (bedrock and bulk soil), Table 2 (soil pore water), Table 3 (stream waters) and in the Appendix (Fig.A1, soil pore water).

4.1. Ge/Si ratios of the bedrock and bulk soils

The forest (Fo) and cropland (Cro) catchment bedrocks have similar Ge/Si ratios (2.25 ± 0.23 and 2.21 ± 0.23 µmol mol^{-1}, respectively) (Fig. 3; Table 1). The Ge/Si ratios of the forest soils vary from 1.68 to 3.04 µmol mol^{-1}. The CroS soils display similar values. In contrast, the CroG soils show distinctively higher Ge/Si ratios (from 2.34 to 3.92 µmol mol^{-1}). Except for the FoS-Top samples, the soil Ge/Si ratio at 55–65 cm (2.47–3.63 µmol mol^{-1}) is always higher than that at 20–30 cm (1.68–2.81 µmol mol^{-1}) (Fig. 3, Table 1). Except FoS-LM, FoS-Bot and FoG-UM, all samples at 20–30 cm display Ge/Si ratios in soils comparable to those measured for the bedrocks. Position in the slope (top, middle, bottom) does not seem to influence the soil Ge/Si ratio, which could have been expected considering the upper positions as an eroding zone and the bottom position as the deposition zone potentially accumulating clay fractions eroded from soils upslope.

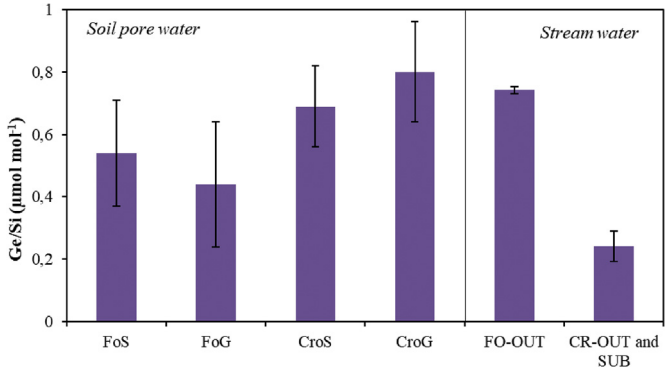

Fig. 4. Average Ge/Si values (± SD) of the soil pore water (left side) and stream waters during base flow (right side). From left to right: soil pore water forest steep (FoS; n = 14), forest gentle (FoG; n = 19), cropland steep (CroS; n = 15), cropland gentle (CroG; n = 13), base flow stream waters forest (FO-OUT; n = 3) and cropland (CR-OUT and CR-SUB; n = 8).

4.2. Ge/Si ratios of the soil pore waters

The Ge/Si ratios of the soil pore waters collected at 70 cm depth vary in the range 0.20–1.07 µmol mol^{-1} (Fig. 3). Except for the FoS-Bot, FoG-Bot and CroT-G sites, the Ge/Si ratios of pore water remained stable over the five-week survey period, ranging from 0.39 to 0.47 and 0.20–0.53 µmol mol^{-1}, respectively, for the forest sites FoS and FoG, and from 0.52 to 0.91 and 0.59–0.96 µmol mol^{-1}, respectively, for the cropland sites CroS and CroG (Fig. 3, Table 2). The pore water Ge/Si ratio at the FoG-Bot site fluctuated (0.53–1.04 µmol mol^{-1}) between each sampling date. Despite these variations, the Ge/Si ratios of the soil pore water under forest (averaged per slope) cannot be distinguished from the Ge/Si ratios of the soil pore water under cropland (Fig. 4).

4.3. Ge/Si ratios of stream waters

4.3.1. Base flow

The Ge/Si ratios of the stream waters during base flow are up to three times higher in the forest catchment (FO-OUT = 0.74 ± 0.01 µmol mol^{-1}, n = 3) than in the cropland catchments (CR-SUB = 0.24 ± 0.03 µmol mol^{-1}, n = 4; CR-OUT = 0.25 ± 0.07 µmol mol^{-1}, n = 4; Fig. 4; Table 3).

4.3.2. Rain events

In forest, the variations of the Ge/Si ratio of stream waters during a rain event seem to be dictated by the influence on the stream discharge: a small increase in discharge (~3 times) resulted in a narrow range of Ge/Si values (0.61–0.76 µmol mol^{-1}; Fig. 5a; Table 3), whereas a larger increase in discharge (~40 times) resulted in a larger range of Ge/Si values in stream waters (from 0.43 to 3.16 µmol mol^{-1}; Fig. 5b; Table 3). More specifically, with a small increase in discharge, the Ge/Si ratio in the stream increased, and then remained constant with Ge/Si values similar to the base flow Ge/Si ratios (0.74 ± 0.01 µmol mol^{-1}; Table 3), whereas with a large increase in discharge, the change in Ge/

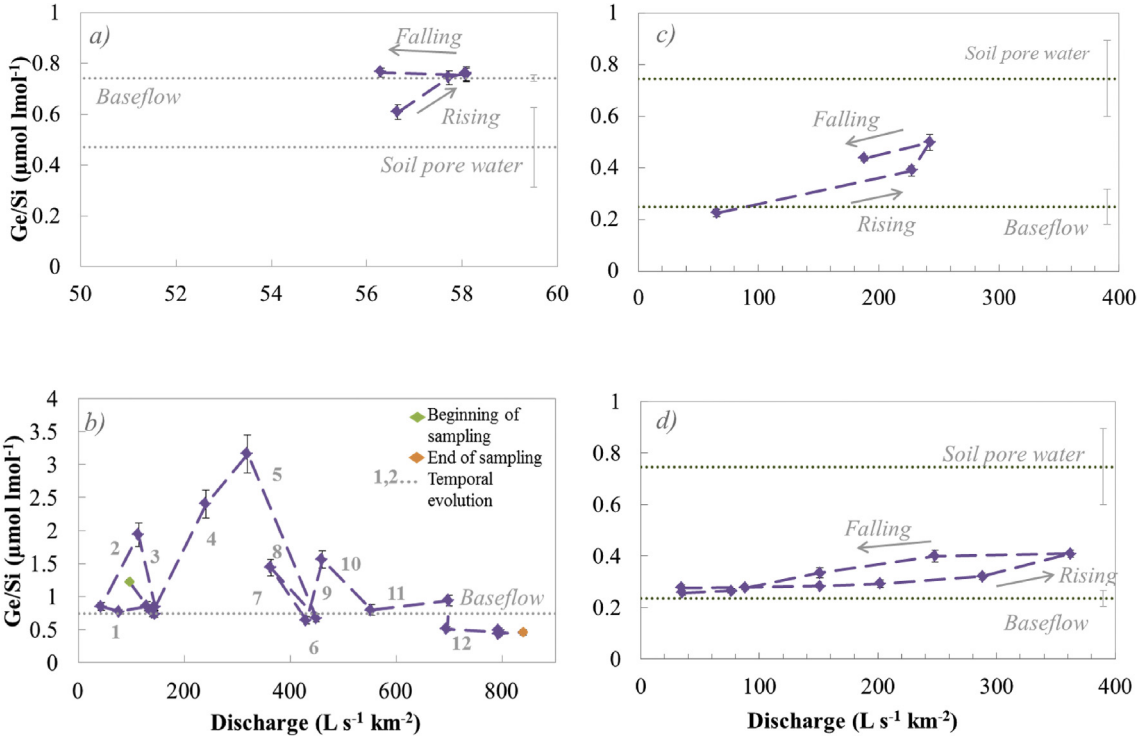

Fig. 5. Evolution of the Ge/Si ratio (± SD) in stream waters with discharge during rain events. a) Forest (FO-OUT) small rain event with a ~3-time increase in discharge, b) forest (FO-OUT) large rain event with a ~40 time increase in discharge (green dot = beginning of sampling; orange dot = end of sampling; numbers = temporal evolution of sampling), c) Cropland whole catchment (CR-OUT) with a ~12 time increase in discharge, d) Cropland sub-catchment (CR-SUB) with a ~38 time increase in discharge. Horizontal dotted lines represent the average Ge/Si ratios (± SD) of the base flow and soil pore water. (For interpretation of the references to colour in this figure legend, the reader is referred to the web version of this article.)

Table 1
Si and Ge concentrations and Ge/Si ratios in bedrocks and bulk soil samples. Bulk soil samples grouped by slope and sorted by slope position from top to bottom. Last line: white material identified in cropland gentle slope.

Slope position	Code	Si mol kg^{-1}	Ge µmol kg^{-1}	Ge/Si µmol mol^{-1}	error Ge/Si µmol mol^{-1}
Bedrock sample	Forest	11	25	2.21	0.23
Bedrock sample	Cropland	12	26	2.25	0.23
Forest steep slope (FoS)					
Top (T)	FoS-Top/20-30	10	29	2.81	0.29
	FoS-Top/55-65	11	28	2.65	0.27
Upper Middle (UM)	FoS-UM/20-30	11	24	2.2	0.23
Lower Middle (LM)	FoS-LM/20-30	12	22	1.77	0.18
	FoS-LM/55-65	10	29	3.03	0.31
Bottom (B)	FoS-Bot/20-30	13	22	1.68	0.17
Forest gentle slope (FoG)					
Top (T)	FoG-Top/20-30	12	23	1.90	0.20
	FoG-Top/55-65	11	26	2.47	0.26
Upper Middle (UM)	FoG-UM/20-30	12	24	2.05	0.21
	FoG-UM/55-65	10	29	3.04	0.32
Lower Middle (LM)	FoG-LM/20-30	13	22	1.72	0.18
	FoG-LM/55-65	11	29	2.71	0.28
Bottom (B)	FoG-Bot/20-30	13	23	1.83	0.19
	FoG-Bot/55-65	11	29	2.75	0.28
Cropland steep slope (CroS)					
Top (T)	CroS-Top/20-30	12	23	1.93	0.20
	CroS-Top/55-65	10	28	2.70	0.28
Middle (M)	CroS-M/20-30	11	21	1.87	0.19
Bottom (B)	CroS-Bot/20-30	12	23	1.95	0.20
	CroS-Bot/55-65	10	28	2.79	0.29
Cropland gentle slope (CroG)					
Top (T)	CroG-Top/20-30	11	27	2.40	0.25
	CroG-Top/55-65	9	33	3.63	0.38
Middle (M)	CroG-M/20-30	11	27	2.36	0.24
	CroG-M/55-65	9	30	3.23	0.33
Bottom (B)	CroG-Bot/20-30	11	26	2.34	0.24
	CroG-Bot/55-65	9	31	3.47	0.36
White material Top (T) 130–140 cm depth	CroG-Top/130-140	7.4	29	3.92	0.40

Table 2
Si and Ge concentrations and Ge/Si ratios in soil pore waters (70 cm depth). Samples divided by land use and slope type and presented for the five sampling weeks. The accumulated rainfall between the sampling weeks is given in Table A4.

Slope position	Sampling week	Ge pmol L^{-1}	Si µmol L^{-1}	Ge/Si µmol mol^{-1}	error Ge/Si µmol mol^{-1}
Forest steep (FoS)					
Top	7-8th Oct.	70	156	0.45	0.05
	14-16th Oct.	61	155	0.39	0.01
	21-23rd Oct.	62	159	0.39	0.02
	28-30th Oct.	68	158	0.43	0.04
	7-8th Nov.	67	162	0.42	0.05
Middle	7-8th Oct.	78	173	0.45	0.03
	14-16th Oct.	69	157	0.44	0.01
	21-23rd Oct.	*No sample*			
	28-30th Oct.	74	168	0.44	0.02
	7-8th Nov.	77	165	0.47	0.01
Bottom	7-8th Oct.	194	220	0.89	0.10
	14-16th Oct.	185	225	0.82	0.03
	21-23rd Oct.	114	213	0.54	0.01
	28-30th Oct.	160	208	0.77	0.03
	7-8th Nov.	154	220	0.70	0.03
Forest gentle (FoG)					
Top	7-8th Oct.	79	286	0.28	0.01
	14-16th Oct.	76	294	0.26	0.02
	21-23rd Oct.	53	261	0.20	0.01
	28-30th Oct.	56	279	0.20	0.01
	7-8th Nov.	67	294	0.23	0.02
Upper middle	7-8th Oct.	89	189	0.47	0.01
	14-16th Oct.	87	187	0.47	0.01
	21-23rd Oct.	62	173	0.36	0.01
	28-30th Oct.	80	190	0.42	0.02
	7-8th Nov.	109	209	0.53	0.03
Lower middle	7-8th Oct.	81	175	0.46	0.03
	14-16th Oct.	80	167	0.48	0.03
	21-23rd Oct.	67	160	0.42	0.04
	28-30th Oct.	75	168	0.45	0.04
	7-8th Nov.	66	173	0.38	0.03
Bottom	7-8th Oct.	95	181	0.53	0.03
	14-16th Oct.	130	125	1.04	0.08
	21-23rd Oct.	49	124	0.40	0.10
	28-30th Oct.	92	117	0.78	0.07
	7-8th Nov.	*No sample*			
Cropland steep (CroS)					
Top	7-8th Oct.	107	141	0.76	0.06
	14-16th Oct.	143	175	0.82	0.04
	21-23rd Oct.	126	165	0.76	0.04
	28-30th Oct.	150	167	0.90	0.04
	7-8th Nov.	169	185	0.91	0.04
Middle	7-8th Oct.	98	160	0.61	0.04
	14-16th Oct.	92	165	0.55	0.03
	21-23rd Oct.	88	152	0.58	0.03
	28-30th Oct.	85	162	0.52	0.03
	7-8th Nov.	99	177	0.56	0.03
Bottom	7-8th Oct.	123	158	0.78	0.04
	14-16th Oct.	113	154	0.74	0.04
	21-23rd Oct.	99	166	0.60	0.03
	28-30th Oct.	104	164	0.64	0.03
	7-8th Nov.	120	172	0.70	0.04
Cropland gentle (CroG)					
Top	7-8th Oct.	81	107	0.75	0.07
	14-16th Oct.	108	101	1.07	0.09
	21-23rd Oct.	77	106	0.73	0.06
	28-30th Oct.	80	106	0.76	0.07
	7-8th Nov.	104	113	0.92	0.07
Middle	7-8th Oct.	*No sample*			
	14-16th Oct.	73	125	0.59	0.05
	21-23rd Oct.	78	128	0.61	0.05
	28-30th Oct.	74	113	0.65	0.06
	7-8th Nov.	77	128	0.60	0.05
Bottom	7-8th Oct.	152	171	0.89	0.04
	14-16th Oct.	148	157	0.94	0.04
	21-23rd Oct.	134	150	0.89	0.04
	28-30th Oct.	140	160	0.87	0.04
	7-8th Nov.	149	154	0.96	0.04

Table 3
Si and Ge concentrations and Ge/Si ratios in stream waters: forest catchment outlet (FO-OUT), cropland sub-catchment (CR-SUB) and cropland whole catchment outlet (CR-OUT). Within each catchment, samples are presented during base flow and rain event. The samples of each rain event are presented in the same order as sampled.

Standardised discharge L s^{-1} Km^{-2}	Moment of sampling	Si µmol L^{-1}	Ge pmol L^{-1}	Ge/Si µmol mol^{-1}	error Ge/Si µmol mol^{-1}
Forest catchment (FO-OUT)					
21	base flow 22nd Oct.	235	175	0.74	0.03
1	base flow 31st Oct.	250	188	0.75	0.01
5	base flow 4th Nov.	253	185	0.73	0.03
57	rain event	218	133	0.61	0.03
58	12th Oct.	252	188	0.74	0.03
58		252	191	0.76	0.03
58		253	192	0.76	0.03
58		251	190	0.75	0.03
56		252	192	0.76	0.02
96	rain event	75	92	1.22	0.03
130	16–17th Oct.	117	100	0.85	0.07
77		182	140	0.77	0.04
43		146	124	0.85	0.06
113		30	59	1.94	0.18
144		129	109	0.85	0.07
144		153	113	0.74	0.06
140		111	84	0.76	0.06
240		30	72	2.40	0.22
319		21	68	3.16	0.29
449		134	91	0.68	0.06
363		61	87	1.44	0.12
430		123	79	0.64	0.06
460		55	86	1.56	0.13
553		43	34	0.79	0.08
699		77	72	0.94	0.08
695		146	74	0.51	0.03
798		161	74	0.46	0.04
793		164	80	0.49	0.03
793		164	71	0.43	0.03
839		160	74	0.46	0.04
Cropland subcatchment (CR-SUB)					
–	base flow 21 Oct.	473	125	0.26	0.02
–	base flow 25 Oct.	528	135	0.26	0.01
11	base flow 30 Oct.	559	125	0.22	0.01
8	base flow 5 Nov.	577	115	0.20	0.01
34	rain event	466	129	0.28	0.01
88	13-14th Oct.	389	108	0.28	0.01
151		376	107	0.28	0.00
202		350	103	0.29	0.01
288		246	79	0.32	0.01
363		215	88	0.41	0.01
248		230	92	0.40	0.02
151		305	102	0.33	0.02
76		425	113	0.27	0.01
35		478	125	0.26	0.01
Cropland whole catchment outlet (CR-OUT)					
–	base flow 21 Oct.	406	136	0.33	0.00
–	base flow 25 Oct.	460	126	0.27	0.02
20	base flow 30 Oct.	495	105	0.21	0.02
16	base flow 5 Nov.	526	95	0.18	0.01
65	rain event	319	72	0.22	0.01
227	13-14th Oct.	260	101	0.39	0.02
242		155	77	0.50	0.03
188		199	87	0.44	0.01

Si ratios in stream waters was random with changing discharge. The Ge/Si ratios in the stream during the said large rain event are generally above the Ge/Si ratio in base flow (Fig. 5b), except after a very high discharge ($\sim 800\,L\,s^{-1}\,km^{-2}$) with a stream Ge/Si ratio lower than base flow values.

In cropland, the Ge/Si ratio in stream waters increases with the rising limb (from 0.22 to 0.50 μmol mol^{-1} for CR-OUT; from 0.28 to 0.41 μmol mol^{-1} for CR-SUB) and decreases with the falling limb (to 0.44 μmol mol^{-1} for CR-OUT, to 0.26 μmol mol^{-1} for CR-SUB) in both catchments (CR-OUT and CR-SUB; Fig. 5c and d; Table 3). At both CR-OUT and CR-SUB, the Ge/Si ratio in streams is higher in the falling limb than in the rising limb for a same discharge value (Fig. 5c and d).

5. Discussion

5.1. Controls on Ge/Si ratios in soils

The Ge/Si ratios measured for the bedrock (2.21–2.25 μmol mol^{-1}) are within the range reported for silicate rocks (Ge/Si = 1–3 μmol mol^{-1}; Bernstein, 1985). The bulk soils display Ge/Si values (1.68–3.63 μmol mol^{-1}) close to or higher than those in the bedrock (Fig. 3). The Ge/Si ratio of the FoS-UM soil sample may reflect the shallow soil depth (50 cm) and proximity of the bedrock to the surface. Preferential incorporation of Ge in clay minerals during weathering typically increases the Ge/Si ratio of soil relative to that in the bedrock (e.g., Bernstein, 1985; Murnane and Stallard, 1990; Froelich et al., 1992). In Hawaii, weathered volcanic soils display Ge/Si ratios that are up to ten times higher than the values of the basaltic parent material, a large increase attributed to high desilication in these soils (Kurtz et al., 2002). In contrast, accumulation of residual quartz with a low Ge/Si ratio (0.5–1 μmol mol^{-1}; Kurtz et al., 2002; Lugolobi et al., 2010) in soils decreases the Ge/Si values. Except the CroG samples, the forest and cropland bulk soils display similar Ge/Si ratios (Fig. 3). We attribute the comparatively high Ge/Si ratios measured in the CroG soils to halloysite, which was clearly identified in the soil profiles (Appendix A1). The soil halloysite has a Ge/Si ratio of 3.92 ± 0.40 μmol mol^{-1}, i.e. higher than that of the bulk soil (Fig. 3).

Similar to previous findings in tropical environments (Kurtz et al., 2002; Lugolobi et al., 2010), the Ge/Si signatures of the forest and cropland bulk soils may be controlled by the presence in various proportions of quartz and clay minerals (as quantified by XRD analysis, Appendix A1, Table A1). These typically display a low and high Ge/Si ratio, respectively. The Ge/Si ratio and the quartz content in the soils are inversely correlated (R = - 0.79, Fig. 6a). In contrast, there is a positive correlation (R = 0.69, Fig. 6b) between the soil Ge/Si ratios and the kaolinite + halloysite contents. Thus, the range of Ge/Si ratio values found for soils probably results from an end-member mixing (Fig. 6c) between quartz and clay minerals. The quartz in soil originates from the rhyodacite parent material of which the mineral assemblage is dominated by quartz (~38%) and sanidine (K-feldspar; ~45–55%), and some traces of hematite and goethite. As soil weathers, clay minerals are formed, increasing the clay content. An accumulation of quartz, (which is resistant to weathering) in soil should deplete the soil in Al relative to the parent material, whereas an accumulation of clay minerals should enrich the soil in Al relative to the parent material (e.g., Al/Si molar ratio of kaolinite at 0.9; Kurtz et al., 2002). Fig. 6c indicates a positive linear correlation between the Ge/Si ratios and Al/Si ratios in the bulk soil samples (Ge/Si = 5.22*Al/Si + 1.09, R = 0.96, the Al/Si ratios are provided in Appendix Table A1). Using this relationship, and assuming an Al/Si ratio of 0 for quartz and 0.9 for kaolinite, their Ge/Si ratio is calculated to be ~1.08 and ~5.79 μmol mol^{-1}, respectively. This is consistent with the Ge/Si ratios reported for quartz (0.5–1 μmol mol^{-1}) and kaolinite (4.8–6.1 μmol mol^{-1}) elsewhere (Kurtz et al., 2002; Lugolobi et al., 2010). Thus, we conclude that the Ge/Si ratios of the cropland and forest soils are controlled by the presence of quartz and clay minerals (such as kaolinite).

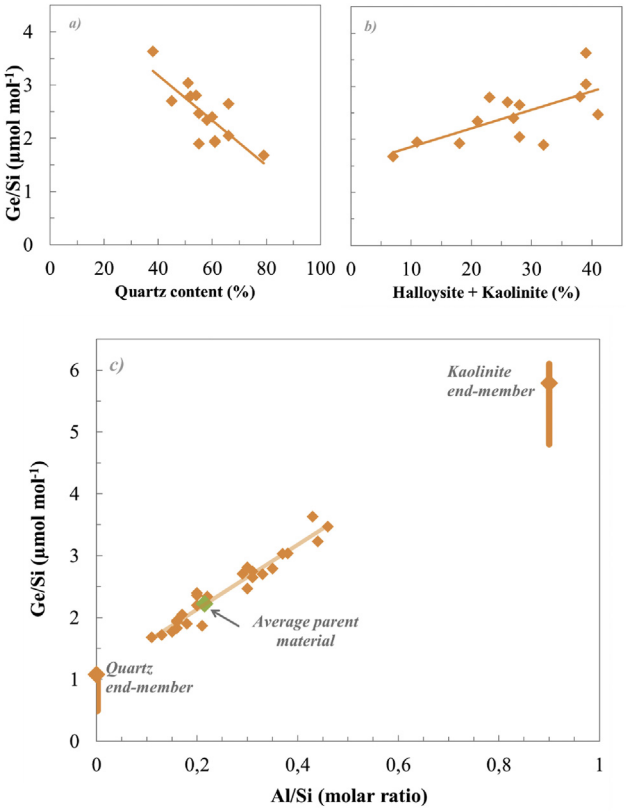

Fig. 6. a) Ge/Si ratios of bulk soils as a function of soil quartz content (R = −0.79, n = 14). b) Ge/Si ratios of the bulk soil as a function of the soil halloysite and kaolinite content (R = 0.69, n = 14). c) Ge/Si ratios as a function of Al/Si (mol mol^{-1}) in bulk soil samples (orange; fitting line: Ge/Si = 5.22*Al/Si + 1.09, R = 0.96, n = 25) and parent material (green; average for both rocks: Al/Si = 0.22, Ge/Si = 2.23 μmol mol^{-1}). End-members obtained from fitting line: quartz (Al/Si typically 0, Ge/Si ~1.09 μmol mol^{-1}); kaolinite (Al/Si typically 0.9, Ge/Si ~5.79 μmol mol^{-1}). Range of Ge/Si ratios from literature: quartz Ge/Si 0.5–1 μmol mol^{-1}; kaolinite Ge/Si 4.8–6.1 μmol mol^{-1} (Kurtz et al., 2002; Lugolobi et al., 2010). (For interpretation of the references to colour in this figure legend, the reader is referred to the web version of this article.)

A potential additional contribution to the Ge/Si in soils relate to the presence of iron oxides and (oxy)hydroxides in soils. The content of iron oxides and (oxy)hydroxides in our soils, as quantified by the dithionite-citrate-bicarbonate extraction method (Fe_d; Mehra and Jackson, 1960), ranges between 13 and 44 g kg^{-1} (Appendix Table A1). It is shown experimentally that Ge adsorbs to the surface of these minerals, and that Ge is likely to be adsorbed more efficiently compared to Si (Bernstein, 1985; Anders et al., 2003; Pokrovsky et al., 2006, 2014), thereby potentially affecting the Ge/Si fractionation. However, this is mainly expected for geological settings such as the emergence of underground reduced waters, the redox barrier near the sediment-water interface, or the top of the hydrothermal plume above hydrothermal vents near oceanic ridges (Pokrovsky et al., 2006). During weathering, it is shown that the precipitation of Fe-oxyhydroxides is not a major factor contributing to Ge/Si fractionation in soils, and that elevated soil Ge/Si ratios reflect the partitioning of Ge into secondary clay minerals (Scribner et al., 2006).

The Ge/Si ratios are lower in the soil pore water samples than in the bulk soils (Fig. 3). This is consistent with preferential incorporation of Ge over Si in clay lattices (e.g., Bernstein, 1985; Murnane and Stallard, 1990; Froelich et al., 1992). Slope position (top, middle, bottom) does not influence the Ge/Si ratio in soil pore water

(0.59 ± 0.22 µmol mol^{-1}), a result consistent with what was observed for the bulk soils (2.45 ± 0.56 µmol mol^{-1}). Exceptions to these observations are the FoS-Bot and FoG-Bot soil pore waters for which the Ge/Si ratios varied (0.4–1.04 µmol mol^{-1}) during the five-week period of sampling. This may reflect inputs of soil colloids transferred from upslope by lateral water flow through soil macroporosity (see section 5.2) (McIntosh et al., 2017). Such materials typically contain high-Ge/Si ratio clay minerals, which may increase the Ge/Si ratio of the soil pore water (Trostle et al., 2016; Aguirre et al., 2017; McIntosh et al., 2017). Contribution from colloids to soil pore water can be heterogeneous given that the rainfall pattern was unevenly distributed over the five weeks of sampling (from no rain between two consecutive samples up to 143 mm rainfall over one week between two consecutive samples; Appendix Table A4). Assuming that lateral water flow through soil macroporosity is higher in a forest catchment compared to cropland (Uchida et al., 2001; Bachmair and Weiler, 2011; Beven and Germann, 2013; see section 5.2), a larger contribution of colloids from upslope to pore water at the bottom of the slope may be expected in forest compared to cropland during rainfall (see section 5.3).

The Ge/Si ratio of soil pore water (average along the slope) under forest cannot be distinguished from that measured for the cropland samples (Fig. 4). Forest conversion to cropland likely alters the biological cycling of Si (Lucas et al., 1993; Struyf et al., 2010) and therefore, one may suspect a change in the Ge/Si ratio of soil pore water in cropland. Silicon-accumulating plants are known to take up Si preferentially over Ge during plant growth, thereby increasing the Ge/Si ratio of soil pore water (e.g., Seyfferth et al., 2013). Among the crops from the studied sites, soybean is a higher Si-accumulator than tobacco (Ma and Takahashi, 2002; Hodson et al., 2005). Thus, a control by plant uptake of the Ge/Si ratio in soil pore water should lead to different Ge/Si values at a spatial scale between sites, and at a temporal scale between the sampling weeks due to plant growth during the sampling campaign. However, this is not the case (Appendix Fig.A1) and thus, the influence of plant uptake on Ge/Si ratio in soil pore water is probably limited. It also appears that, even if the stock of biogenic silica in the studied soils decreases under cropland steep slope relative to the forest (Unzué-Belmonte et al., 2017), the Ge/Si ratio of the soil pore water under cropland steep slope is not different than that of the other three slopes. Consequently, biogenic silica does not seem to be a main control on the Ge/Si ratios in pore water. Another influence of deforestation on the Ge/Si ratios in soil pore water could have been expected due to increased erosion (Montgomery, 2007), exposing less weathered minerals to weathering (Millot et al., 2002). Erosion and transport of sediments in rivers in the cropland catchment of Arvorezinha increase during intense rainfall (Merten and Minella, 2006). Removal of the surface soil layer by erosive processes may expose less weathered mineral surfaces to weathering and thereby, contribute to release Si over Ge in solution (while Ge is sequestered in clay minerals), which would decrease the Ge/Si of pore water. However, the Ge/Si ratio of the pore water under cropland is not different than that measured for the forest catchment. Thus, there is no evidence that primary mineral weathering is enhanced in cropland soils. Overall, clay formation and colloidal contribution are likely the main controlling factors on the Ge/Si ratios in pore water for the sampling period considered.

5.2. Stream waters Ge/Si ratios in base flow point to deeper weathering in cropland than in forest

While the pore water samples in the forest and cropland soils display comparable Ge/Si ratios, the stream waters in base flow from the cropland catchment are characterised by lower average Ge/Si values (0.24 ± 0.05 µmol mol^{-1}) than those measured in the forest catchment (0.74 ± 0.01 µmol mol^{-1}) (Fig. 4). The composition of stream waters in base flow is known to reflect groundwater chemistry (e.g., Bishop et al., 1990; Robson et al., 1992; Peters and Ratcliffe, 1998; Burns et al., 2001; Kurtz et al., 2011). Therefore, different Ge/Si ratios in the forest and cropland stream waters in base flow suggest distinct controlling factors of groundwater chemistry.

Topography (gentle slopes of 9 ± 2°, and steep slopes of 15 ± 3°) and climatic conditions are comparable between the forest and cropland catchments. Therefore, differences in landscape and climatic influences on water transfer in soils down to groundwater between catchments are probably limited (Zapata-Rios et al., 2015). Difference in size between the forest (FO-OUT = 0.03 km^2) and cropland (CR-OUT = 1.19 km^2; CR-SUB = 0.14 km^2) catchments could influence the length of the water pathway to groundwater and therefore, the Ge/Si ratio in stream waters in base flow. However, the Ge/Si ratio in stream waters in base flow is noticeably higher in the forest catchment (FO-OUT = 0.74 ± 0.01 µmol mol^{-1}) compared to the values found for both the whole (CR-OUT = 0.25 ± 0.07 µmol mol^{-1}; 40 times larger in size than the forest catchment) and sub- (CR-SUB = 0.24 ± 0.03 µmol mol^{-1}; 5 times larger in size than the forest catchment) cropland catchments. In addition, in the cropland whole catchment, despite being characterised by a size that is nine times larger than the sub-catchment, the Ge/Si ratio in stream waters in base flow is similar in both outlets (CR-OUT = 0.25 ± 0.07 µmol mol^{-1} and CR-SUB = 0.24 ± 0.03 µmol mol^{-1}). Therefore, catchment size cannot explain the discrepancy in the Ge/Si ratio values determined for stream waters in base flow in the forest and cropland catchments. Further investigations should consider a comparison of larger forested and cropland catchments to verify if the observed trend can be extrapolated at different catchment sizes.

A lower Ge/Si ratio in stream waters in base flow in cropland may result from a contribution of phytolith dissolution. According to previous works, the Ge/Si ratio of phytoliths range from 0.03 to 0.50 µmol mol^{-1} (e.g., Derry et al., 2005; Blecker et al., 2007; Lugolobi et al., 2010). The soils with the highest phytolith content correspond to CroG (Unzué-Belmonte et al., 2017); they display a Ge/Si ratio in pore water greater than 0.50 µmol mol^{-1}, a value incompatible with phytolith dissolution. On this basis, a contribution from phytolith dissolution to explain the groundwater Ge/Si ratio is dismissed.

A lower Ge/Si ratio in stream waters in base flow in cropland may also result from secondary clay mineral precipitation, a process which depletes Ge in the solution (e.g., Bernstein, 1985; Murnane and Stallard, 1990; Froelich et al., 1992). Conversely, clay mineral dissolution enriches the solution in Ge and increases the Ge/Si ratio. Forests are systems characterised by elevated soil macroporosity associated to roots and biological activity (e.g., Aubertin, 1971; Beasley, 1976; Edwards and Lofty, 1977) allowing lateral water pathways (e.g., Beven and Germann, 1982; McDonnell, 1990; Uchida et al., 2001; Bachmair and Weiler, 2011; Beven and Germann, 2013). Soil bulk density from the forest site displays a general increase in values with depth (Appendix Figs. A2 a, b), and comparatively limited changes with depth in cropland relative to forest (Appendix Figs. A2 c, d). Although more analyses would be required to link these changes to soil macroporosity in surface horizons, we hypothesise that soil compaction (e.g., Soane and van Ouwerkerk, 1994) and removal of the upper soil cover by erosion associated to agricultural practices (e.g., Montgomery, 2007) altered soil macroposity and thereby, soil structure, in the cropland catchment. Preferential lateral water flows through soil macroporosity in surface horizons (above 30 cm) are thought to limit water percolation in soils in forest relative to cropland (Robinet et al., 2018). Water percolation is also likely to be more limited in forest relative to cropland due to higher evapotranspiration in forests compared to croplands (e.g., Foley et al., 2003). This is supported by increased base flow discharge reported after deforestation (e.g.,Costa et al., 2003; Brown et al., 2005; Molina et al., 2012). Further, water uptake by roots limits deep drainage in forest soils relative to cropland (Lucas, 2001). Predominance of lateral water flow through macroporosity, higher evapotranspiration, and roots uptake are expected to result in limited water percolation under forest, and comparatively higher water percolation in cropland. Water renewal in groundwater would be reduced under forest, thereby increasing

water residence time in the groundwater reservoir under forest. In turn, this may favour dissolution of clay minerals, and produce Ge/Si values in stream waters in base flow (0.74 ± 0.01 μmol mol^{-1}) within the range of the Ge/Si ratio in soil pore water (0.20–1.04 μmol mol^{-1}). In contrast, higher water percolation under cropland relative to forest is likely to increase water renewal in the deeper soil layers, thus favouring weathering (Chabaux et al., 2017) and incorporation of Ge in newly-formed clay minerals. This would generate lower Ge/Si ratio in groundwater, as reflected by the lower Ge/Si ratio in stream waters in base flow under cropland (0.24 ± 0.05 μmol mol^{-1}) relative to forest.

5.3. Stream waters Ge/Si ratios during a rain event support a deeper source of element fluxes in cropland than in forest

At the forest catchment, Fig. 5a shows that a small increase in discharge (threefold, i.e., during a small rain event) slightly decreased stream Ge/Si values (0.61 μmol mol^{-1}) relative to those measured in base flow (0.74 ± 0.01 μmol mol^{-1}; Fig. 4). Lateral water fluxes from soil pore water are favoured by macroporosity under forest (section 5.2; Robinet et al., 2018): a contribution from soil pore water (under forest: 0.48 ± 0.19 μmol mol^{-1}) may explain a temporary decrease in the Ge/Si ratio of the stream waters relative to the base flow Ge/Si values. For a major rain event with ~40 times increase in discharge, the Ge/Si ratio in stream waters increases and decreases rapidly relative to Ge/Si values in base flow, with no specific trend with increasing discharge (Fig. 5b). The contrast in Ge/Si ratio in stream waters between the small and the major rain events relative to base flow (Fig. 5a and b) confirms the importance to sample in contrasted hydrological conditions (Schaffhauser et al., 2014) to better understand the controls on Ge/Si ratios in stream waters. Discrete zones of element mobilisation within soils and sediments can lead to discrete pulses of a particular solute into streams (McClain et al., 2003; Andrews et al., 2011; Herndon et al., 2015). This may result in pulses of high Ge/Si ratios during the rain event. Moreover, erosion and mobilisation of soils with clay minerals (characterised by high Ge/Si ratios) by runoff contributing to high discharge (and high turbidity) can increase the Ge/Si ratio of stream waters through the presence of colloids in the dissolved fraction filtered at 0.45 μm (Aguirre et al., 2017). Such runoff (known as saturation overland flow) during rain events is well documented in tropical forests (Bonell, 2005). A mobilisation from soils is also indicated by the variability of the Ge/Si ratios observed in soil pore water at the FoG at the bottom of the slope, i.e. the portion of the slope where colloids are transferred from upslope by lateral water flow through soil macroporosity and accumulate (0.4–1.04 μmol mol^{-1}, Table 2; over 5 sampling weeks with distinct rainfall amounts between the weeks, Appendix Table A4).

Under cropland, during a rain event, the Ge/Si ratio in stream waters (both at CR-OUT and CR-SUB) increases during the rising limb relative to the base flow Ge/Si values and decreases during the falling limb to reach base flow Ge/Si values. Overall, the Ge/Si values during the falling limb are higher than during the rising limb for a similar discharge (Fig. 5c and d). This evolution cannot be explained by dilution with increasing discharge because Si concentration decreases almost twofold faster than Ge concentration with increasing discharge (Appendix Fig.A3). The evolution is characterised by a « hysteresis » loop, similar to the evolution of intra-storm Si concentrations in streams (Wels et al., 1991; Hinton et al., 1994; Evans and Davies, 1998; Hornberger et al., 2001; Scanlon et al., 2001). Such behaviour is typically observed when two or more sources of water are mixed in different proportions (Kurtz et al., 2011). This observation supports a contribution from an additional source of chemical element fluxes to streams during a rain event (DeWalle et al., 1988; Bazemore et al., 1994; Rice and Hornberger, 1998; Klaus and McDonnell, 2013). Soil pore water mobilised during rainfall events may contribute to streams, along with groundwater input (McGlynn and McDonnell, 2003; Godsey et al., 2009; Kurtz et al., 2011; Herndon et al., 2015). A contribution from soil pore water (with Ge/Si values 0.52–1.07 μmol mol^{-1}; Table 2) to streams would increase the stream Ge/Si ratios during a rain event relative to the value in base flow (Kurtz et al., 2011). This is consistent with our observations (Fig. 7). The change observed in Ge/Si ratio of cropland stream water during a rain event in reference to base flow confirms that stream water composition is controlled by distinct processes in cropland compared to those operating under forest cover (see section 5.2).

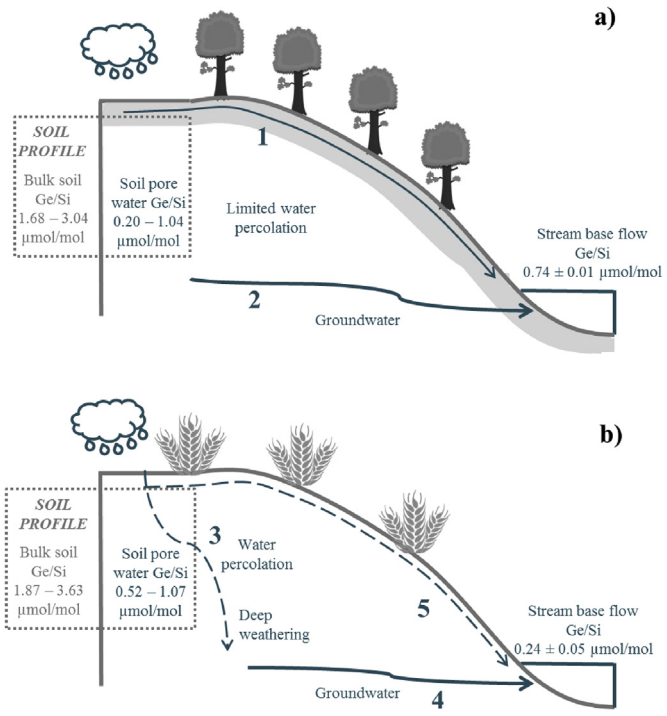

Fig. 7. Conceptual schematic to explain the differences in water percolation between forest and cropland. a) In forest the macroporosity of the surface soils (represented by the grey layer below the soil surface) favours lateral water flow downslope (1) and limits percolation downwards the soil profile. Water renewal in groundwater (2) is limited and the higher water residence time may allow clay dissolution and results in Ge/Si ratio in stream waters in base flow within the range of Ge/Si ratio in soil pore water. b) In cropland the changes in the water flow path induced by forest conversion result in higher water percolation (3), consequently water can reach deeper material, as a result, the composition of the groundwater (4) reflects mineral weathering and clay formation leading to lower Ge/Si ratio in stream waters in base flow than in forest. During a rain event, soil pore water may be mobilised from the soil profile and contribute to the stream by runoff (5).

6. Conclusions

The Ge/Si ratio was used as a weathering tracer to understand changes in mineral weathering contribution to solutes export to streams following a recent forest conversion to cropland (~100 years, Brazil). The Ge/Si ratios measured in bedrock, soils, soil pore water, streams in base flow and streams during a rain event point to a modification of the location of the weathering processes generating element fluxes exported towards rivers after forest conversion to cropland. It is hypothesised that under forest, preferential lateral water fluxes and higher evapotranspiration reduce water percolation in soils relative to cropland. Higher percolation in cropland favours weathering and incorporation of Ge in newly-formed clay minerals by increasing water renewal in the deeper soil layers, and lowers Ge/Si ratio in groundwater, as reflected by lower Ge/Si ratio in stream waters during base flow in cropland relative to forest. The change in stream waters Ge/Si ratio during a rain event in reference to base flow confirms that stream water composition is controlled by distinct processes in cropland than

under forest. This study highlights that studying the impact of forest conversion on soils requires considering not only the pedon scale (where changes in mineral weathering contribution to soil pore water after forest conversion were not observable), but also the catchment scale integrating the response of the system to a perturbation of the soil surface.

Acknowledgements

We are grateful to the staff from the Soils Department of Universidade Federal de Santa Maria for logistic and technical support during the sampling campaign (A. Schlesner, C. Barros, R. Ramon, L. Ávila). We thank the team in the Department of Earth and Atmospheric Sciences of Cornell University for their help during the Ge measurements (G. McElwee, A. Aguirre, K. Grant, A. Pérez Fodich). We thank A. Iserentant from UCL for help with the Si measurements. The manuscript benefited from discussions with J.T. Cornelis, V. Vanacker, and D. Houben. We thank the editor and the anonymous reviewers for their constructive comments to improve the manuscript. Y.A.M. and J.R. are funded by the Belgian Science Policy Office (BELSPO) in the framework of the Inter University Attraction Pole project (P7/24): SOGLO – The soil system under global change. Y.A.M benefited from the IAGC PhD Student Grant 2015 for this research. S.O. is funded by the "Fonds National de la Recherche Scientifique" (FNRS, Belgium, FC69480). Partial support for work at Cornell University was provided by NSF 1349269.

Appendix A. Supplementary data

Supplementary data related to this article can be found at doi:http://dx.doi.org/10.1016/j.apgeochem.2018.06.002.

References

Aguirre, A.A., Derry, L.A., Mills, T.J., Anderson, S.P., 2017. Colloidal transport in the Gordon Gulch catchment of the Boulder Creek CZO and its effect on C-Q relationships for silicon. Water Resour. Res. 53, 2368–2383.

Alexandre, A., Meunier, J.-D., Colin, F., Koud, J.-M., 1997. Plant impact on the biogeochemical cycle of silicon and related weathering processes. Geochem. Cosmochim. Acta 61, 677–682.

Ameijeiras-Mariño Y., Opfergelt S., Cornélis J.-T., Vanacker V., Minella J.P.G., Lamouline F., Vermeire M.-L., Campforts B., Van de Broek M., Delmelle P. Influence of forest conversion to cropland on soil weathering degree in Southern Brazil. Catena (under revision).

Anders, A.M., Sletten, R.S., Derry, L.A., Hallet, B., 2003. Germanium/silicon ratios in the Copper River Basin, Alaska: weathering and partitioning in periglacial versus glacial environments. J. Geophys. Res. 108. http://dx.doi.org/10.1029/2003JF000026.

Andrews, D.M., Lin, H., Zhu, Q., Jin, L., Brantley, S.L., 2011. Hot spots and hot moments of dissolved organic carbon export and soil organic carbon storage in the Shale Hills catchment. Vadose Zone J. 10, 943–954.

Aubertin, G.M., 1971. Nature and Extent of Macropores in forest Soils and Their Influence on Subsurface Water Movement. Northeastern Forest Experiment Station, Forest Service US Department of Agriculture, Upper Darby, Pennsylvania.

Bachmair, S., Weiler, M., 2011. New dimensions of hillslope hydrology. In forest hydrology and biogeochemistry. Synthesis Past Res. Future Direct. 455–481.

Bazemore, D.E., Eshleman, K.N., Hollenbeck, K.J., 1994. The role of soil water in storm flow generation in a forested headwater catchment: synthesis of natural tracer and hydrometric evidence. J. Hydrol. 162, 47–75.

Beasley, R.S., 1976. Contribution of subsurface flow from the upper slopes of forested watersheds to channel flow. Soil Sci. Soc. Am. J. 40, 955–957.

Bellieni, G., Comin-Chiaramonti, P., Marques, L., Melfi, A., Nardy, A., Papatrechas, C., Piccirillo, E., Roisenberg, A., Stolfa, D., 1986. Petrogenetic aspects of acid and basaltic lavas from the Paraná plateau (Brazil): geological, mineralogical and petrochemical relationships. J. Petrol. 27 (4), 915–944.

Bernstein, L.R., 1985. Germanium geochemistry and mineralogy. Geochem. Cosmochim. Acta 49, 2409–2422.

Beven, K., Germann, P., 1982. Macropores and water flow in soils. Water Resour. Res. 18, 1311–1325.

Beven, K., Germann, P., 2013. Macropores and water flow in soils revisited. Water Resour. Res. 49, 3071–3092.

Bishop, K.H., Grip, H., O'Neill, A., 1990. The origins of acid runoff in a hillslope during storm events. J. Hydrol. 116, 35–61.

Blecker, S.W., King, S.L., Derry, L.A., Chadwick, O.A., Ippolito, J.A., Kelly, E.F., 2007. The ratio of germanium to silicon in plant phytoliths: quantification of biological discrimination under controlled experimental conditions. Biogeochemistry 6, 189–199.

Bonell, M., 2005. Chapter 14. Runoff generation in tropical forests. In: Bonell, M., Bruijnzeel, L. (Eds.), Forests, Water and People in the Humid Tropics: Past, Present and Future Hydrological Research for Integrated Land and Water Management (International Hydrology Series. Cambridge University, Cambridge, pp. 314–406.

Brown, A.E., Zhang, L., McMahon, T.A., Western, A.W., Vertessy, R.A., 2005. A review of paired catchment studies for determining changes in water yield resulting from alterations in vegetation. J. Hydrol. 310, 28–61.

Burns, D.A., McDonnell, J.J., Hooper, R.P., Peters, N.E., Freer, J.E., Kendall, C., Beven, K., 2001. Quantifying contributions to storm runoff through end-member mixing analysis and hydrologic measurements at the Panola Mountain Research Watershed (Georgia, USA). Hydrol. Process. 15, 1903–1924.

Carey, J.C., Fulweiler, R.W., 2012. Human activities directly alter watershed dissolved silica fluxes. Biogeochemistry 111, 125–138.

Chabaux, F., Viville, D., Lucas, Y., Ackerer, J., Ranchoux, C., Bosia, C., Pierret, M.C., Labasque, T., Aquilina, L., Wyns, R., Lerouge, C., Dezaye, C., Négrel, P., 2017. Geochemical tracing and modeling of surface and deep water–rock interactions in elementary granitic watersheds (Strengbach and Ringelbach CZOs, France). Acta Geochim. http://dx.doi.org/10.1007/s11631-017-0163-5.

Chao, T.T., Sanzolone, R.F., 1992. Decomposition techniques. J. Geochem. Explor. 44, 65–106.

Conley, D.J., Likens, G.E., Buso, D.C., Saccone, L., Bailey, S.W., Johnson, C.E., 2008. Deforestation causes increased dissolved silicate losses in the hubbard brook experimental forest. Global Change Biol. 14, 2548–2554.

Cornélis, J.-T., Delvaux, B., Georg, R.B., Lucas, Y., Ranger, J., Opfergelt, S., 2011. Tracing the origin of dissolved silicon transferred from various soil-plant systems towards rivers: a review. Biogeosciences 8, 89–112.

Costa, M.H., Botta, A., Cardille, J.A., 2003. Effects of large-scale changes in land cover on the discharge of the Tocantins River, Southeastern Amazonia. J. Hydrol. 283, 206–217.

Derry, L.A., Kurtz, A.C., Ziegler, K., Chadwick, O.A., 2005. Biological control of terrestrial silica cycling and export fluxes to watersheds. Lett. Nature 433, 728–731.

DeWalle, D.R., Swistock, B.R., Sharpe, W.E., 1988. Three component tracer model for stormflow on a small Appalachian forested catchment. J. Hydrol 104, 301–310.

Dixon, J.L., Heimsath, A.M., Amundson, R., 2009. The critical role of climate and saprolite weathering in landscape evolution. Earth Surf. Process. Landforms 34, 1507–1521.

Drever, J.I., 1994. The effect of land plants on weathering rates of silicate minerals. Geochem. Cosmochim. Acta 58, 2325–2332.

Edwards, C.A., Lofty, J.R., 1977. Biology of Earthworms, second ed. Chapman and Hall, London, UK.

Evans, C., Davies, T.D., 1998. Causes of concentration/discharge hysteresis and its potential as a tool for analysis of episode hydrochemistry. Water Resour. Res. 34, 129–137.

Ferrier, K.L., Kirchner, J.W., Finkel, R.C., 2012. Weak influences of climate and mineral supply rates on chemical erosion rates: measurements along two altitudinal transects in the Idaho Batholith. J. Geophys. Res. Earth Surf. 117 F02026.

Foley, J.A., 2011. Can we feed the world & sustain the planet? Sci. Am. 305, 60–65.

Foley, J.A., Costa, M.H., Delire, C., Ramankutty, N., Snyder, P., 2003. Green surprise? How terrestrial ecosystems could affect earth's climate. Front. Ecol. Environ. 1, 38–44.

Foley, J.A., DeFries, R., Asner, G.P., Barford, C., Bonan, G., Carpenter, S.R., Chapin, F.S., Coe, M.T., Daily, G.C., Gibbs, H.K., Helkowski, J.H., Holloway, T., Howard, E.A., Kucharik, C.J., Monfreda, C., Patz, J.A., Prentice, I.C., Ramankutty, N., Snyder, P.K., 2005. Global consequences of land use. Science 309, 570–574.

Froelich, P.N., Blanc, V., Mortlock, R.A., Chillrud, S.N., Dunstan, W., Udomkit, A., Peng, T.H., 1992. River fluxes of dissolved silica to the ocean were higher during glacials: Ge/Si in diatoms, rivers and oceans. Paleoceanography 7, 739–768.

Gaillardet, J., Dupré, B., Louvat, P., Allègre, C.J., 1999. Global silicate weathering and CO_2 consumption rates deduced from the chemistry of large rivers. Chem. Geol. 159, 3–30.

Godfray, H.C.J., Beddington, J.R., Crute, I.R., Haddad, L., Lawrence, D., Muir, J.F., Pretty, J., Robinson, S., Thomas, S.M., Toulmin, C., 2010. Food security: the challenge of feeding 9 billion people. Science 327, 812–818.

Godsey, S.E., Kirchner, J.W., Clow, D.W., 2009. Concentration–discharge relationships reflect chemostatic characteristics of US catchments. Hydrol. Process. 23, 1844–1864.

Goudie, A.S., Viles, H.A., 2012. Weathering and the global carbon cycle: geomorphological perspectives. Earth Sci. Rev. 113, 59–71.

Herndon, E.M., Dere, A.L., Sullivan, P.L., Norris, D., Reynolds, B., Brantley, S.L., 2015. Landscape heterogeneity drives contrasting concentration–discharge relationships in shale headwater catchments. Hydrol. Earth Syst. Sci. 19, 3333–3347.

Hinton, M.J., Schiff, L.S., English, M.C., 1994. Examining the contributions of glacial till water to storm runoff using two- and three component hydrograph separations. Water Resour. Res. 30, 983–993.

Hodson, M.J., White, P.J., Mead, A., Broadley, M.R., 2005. Phylogenetic variation in the silicon composition of plants. Ann. Bot. 96, 1027–1046.

Hornberger, G.H., Scanlon, T.M., Raffensperger, J.P., 2001. Modelling transport of dissolved silica in a forested headwater catchment: the effect of hydrological and chemical time scales on hysteresis on the concentration-discharge relationship. Hydrol. Process. 15, 2029–2038.

IUSS Working Group WRB, 2007. World Reference Base for Soil Resources 2006, First Update 2007. World Soil Resources Reports 103. FAO, Rome.

Jacobson, A.D., Blum, J.D., Chamberlain, C.P., Craw, D., Koons, P.O., 2003. Climatic and tectonic controls on chemical weathering in the New Zealand Southern Alps. Geochem. Cosmochim. Acta 67, 29–46.

Kipphardt, H., Valkiers, S., Henriksen, F., De Bièvre, P., Taylor, P.D.P., Tölg, G., 1999. Measurement of the isotopic composition of germanium using GeF4 produced by

direct fluorination and wet chemical procedures. Int. J. Mass Spectrom. 189, 27–37.
Klaus, J., McDonnell, J.J., 2013. Hydrograph separation using stable isotopes: review and evaluation. J. Hydrol. 505, 47–64.
Kurtz, A.C., Derry, L.A., Chadwick, O.A., 2002. Germanium-silicon fractionation in the weathering environment. Geochem. Cosmochim. Acta 66, 1525–1537.
Kurtz, A.C., Lugolobi, F., Salvucci, G., 2011. Germanium-silicon as a flow path tracer: application to the Rio Icacos watershed. Water Resour. Res. 47. https://doi.org/10.1029/2010WR009853.
Lopes, F., 2006. Utilização do modelo Century para avaliar a dinâmica do carbono do solo em uma pequena bacia hidrográfica rural. Master Dissertation. Universidade Federal do Rio Grande do Sul, Porto Alegre.
Lucas, Y., 2001. The role of plants in controlling rates and products of weathering: importance of biological pumping. Annu. Rev. Earth Planet Sci. 29, 135–163.
Lucas, Y., Luizao, F.J., Chauvel, A., Rouiller, J., Nahon, D., 1993. The relation between biological activity of the rain forest and mineral composition of soils. Science 260, 521–523.
Lugolobi, F., Kurtz, A.C., Derry, L.A., 2010. Germanium–Silicon fractionation in a tropical, granitic weathering environment. Geochem. Cosmochim. Acta 74, 1294–1308.
Ma, J.F., Takahashi, E., 2002. Soil, Fertilizer, and Plant Silicon Research in Japan. Elsevier, The Netherlands.
Maher, K., 2010. The dependence of chemical weathering rates on fluid residence time. Earth Planet Sci. Lett. 294, 101–110.
McClain, M.E., Boyer, E.W., Dent, C.L., Gergel, S.E., Grimm, N.B., Groffman, P.M., Hart, S.C., Harvey, J.W., Johnston, C.A., Mayorga, E., McDowell, W.H., Pinay, G., 2003. Biogeochemical hot spots and hot moments at the interface of terrestrial and aquatic ecosystems. Ecosystems 6, 301–312.
McDonnell, J.J., 1990. A rationale for old water discharge through macropores in a steep, humid catchment. Water Resour. Res. 26, 2821–2832.
McGlynn, B.L., McDonnell, J.J., 2003. Role of discrete landscape units in controlling catchment dissolved organic carbon dynamics. Water Resour. Res. 39, 1090–1108.
McIntosh, J.C., Schaumberg, C., Perdrial, J., Harpold, A., Vázquez-Ortega, A., Rasmussen, C., Vinson, D., Zapata-Rios, X., Brooks, P.D., Meixner, T., Pelletier, J., Derry, L., Chorover, J., 2017. Geochemical evolution of the critical zone across variable time scales informs concentration-discharge relationships: jemez river basin critical zone observatory. Water Resour. Res. 53, 4169–4196.
Meade, R.H., Yuzyk, T.R., Day, T.J., 1990. Movement and storage of sediments in rivers of the United States and Canada. In: Wolman, M.G., Riggs, H.C. (Eds.), Surface Water Hydrology. The Geology of North America. Geological Society of America, pp. 255–280.
Mehra, O.P., Jackson, M.L., 1960. Iron oxide removal from soils and clays by a dithionite-citrate system buffered with sodium bicarbonate. In: Proc. 7th Natl. Conf. Clays Clay Minerals, Washington, pp. 317–327.
Merten, G.H., Minella, J.P.G., 2006. Impact on sediment yield caused by intensification of tobacco production in a catchment in southern Brazil. In: Walling, D.E., Horowitz, A.J. (Eds.), Sediment Budgets 2, IAHS Publ. 291. IAHS Press, Wallingford, UK, pp. 239–244.
Millot, R., Gaillardet, J., Dupré, B., Allegre, C.J., 2002. The global control of silicate weathering rates and the coupling with physical erosion: new insights from rivers of the Canadian shield. Earth Planet Sci. Lett. 196, 83–98.
Minella, J.P.G., 2003. Identificação de fontes de produção de sedimentos em uma pequena bacia rural. (Identification of sediment sources in a small rural drainage basin.) Dissertacão de Mestrado – programa de Pós-Graduação em Recursos Hídricos e Saneamento Ambiental. Instituto de Pesquisas Hidráulicas. Universidade Federal do Rio Grande do Sul 89.
Minella, J.P.G., Walling, D.E., Merten, G.H., 2008. Combining traditional monitoring and sediment source tracing techniques to assess the impact of improved land management on catchment sediment yields. J. Hydrol. 348, 546–563.
Minella, J.P.G., Walling, D.E., Merten, G.H., 2014. Establishing a sediment budget for a small agricultural catchmentin southern Brazil, to support the development of effective sediment management strategies. J. Hydrol. 519, 2189–2201.
Molina, A., Vanacker, V., Balthazar, V., Mora, D., Govers, G., 2012. Complex land cover change, water and sediment yield in a degraded Andean environment. J. Hydrol 472–473, 25–35.
Montanheiro, T.J., Yamamoto, J.K., Kihara, Y., 2004. Serra geral formation—são paulo state, Brazil: a potential source for natural pozzolans. Mater. Lett. 58 (6), 876–881.
Montgomery, D.R., 2007. Soil erosion and agricultural sustainability. P. Natl. Acad. Sci. USA 104, 13268–13272.
Moon, S., Chamberlain, C.P., Hilley, G.E., 2014. New estimates of silicate weathering rates and their uncertainties in global rivers. Geochem. Cosmochim. Acta 134, 257–274.
Mortlock, R.A., Froelich, P.N., 1987. Continental weathering of germanium: Ge/Si in the global river discharge. Geochem. Cosmochim. Acta 51, 2075–2082.
Mortlock, R.A., Froelich, P.N., 1996. Determination of germanium by isotope dilution-hydride generation inductively coupled plasma mass spectrometry. Anal. Chem. Acta 332, 277–284.
Murnane, R.J., Stallard, R.F., 1990. Germanium and silicon in rivers of the Orinoco drainage basin. Nature 44, 749–752.
Peters, N.E., Ratcliffe, E.B., 1998. Tracing hydrologic pathways using chloride at the panola mountain research watershed, Georgia, USA. Water, Air, Soil Pollut. 105, 263–275.
Pimentel, D., 2006. Soil erosion: a food and environmental threat. Environ. Dev. Sustain. 8, 119–137.
Pokrovsky, O.S., Pokrovski, G.S., Schott, J., Galy, A., 2006. Experimental study of germanium adsorption on goethite and germanium coprecipitation with iron hydroxide: X-ray absorption fine structure and macroscopic characterization. Geochem. Cosmochim. Acta 70, 3325–3341.
Pokrovsky, O.S., Galy, A., Schott, J., Pokrovski, G.S., Mantoura, S., 2014. Germanium isotope fractionation during Ge adsorption on goethite and its coprecipitation with Fe oxy(hydr)oxides. Geochem. Cosmochim. Acta 131, 138–149.
Quinton, J.N., Govers, G., Van Oost, K., Bardgett, R., 2010. The impact of agricultural erosion on biogeochemical cycling. Nat. Geosci. 3, 311–314.
Ramon, R., Minella, J.P.G., Merten, G.H., Barros, C.A.P., Canale, T., 2017. Kinetic energy estimation by rainfall intensity and its usefulness in predicting hydro-sedimentological variables in a small rural catchment in southern Brazil. Catena 148, 176–184.
Rasmussen, C., Brantley, S., Richter, D.D., Blum, A., Dixon, J., White, A.F., 2011. Strong climate and tectonic control on plagioclase weathering in granitic terrain. Earth Planet Sci. Lett. 301, 521–530.
Rice, K.C., Hornberger, G.M., 1998. Comparison of hydrochemical tracers to estimate source contributions to peak flow in a small, forested, headwater catchment. Water Resour. Res. 37, 1755–1766.
Robinet, J., Minella, J.P.G., de Barros, C.A.P., Schlesner, A., Lücke, A., Ameijeiras-Mariño, Y., Opfergelt, S., Vanderborght, J., Govers, G., 2018. Impacts of forest conversion and agriculture practices on water pathways in Southern Brazil. Hydrol. Proces. http://dx.doi.org/10.1002/hyp.13155.
Robson, A., Beven, K., Neal, C., 1992. Towards identifying sources of subsurface flow: a comparison of components identified by a physically based runoff model and those determined by chemical mixing techniques. Hydrol. Process. 6, 199–214.
Scanlon, T.M., Raffensperger, J.P., Hornberger, G.M., 2001. Modelling transport of dissolved silica in a forested headwater catchment: implications for defining the hydrochemical response of observed flow pathways. Water Resour. Res. 37, 1071–1082.
Schaffhauser, T., Chabaux, F., Ambroise, B., Lucas, Y., Stille, P., Reuschlé, T., Perrone, T., Fritz, B., 2014. Geochemical and isotopic (U, Sr) tracing of water pathways in the granitic Ringelbach catchment (Vosges Mountains, France). Chem. Geol. 374–375, 117–127.
Schoonejans, J., Vanacker, V., Opfergelt, S., Christl, M., 2017. Long-term soil erosion derived from in-situ ^{10}Be and inventories of meteoric ^{10}Be in deeply weathered soils in southern Brazil. Chem. Geol. 466, 380–388.
Scribner, A.M., Kurtz, A.C., Chadwick, O.A., 2006. Germanium sequestration by soil: targeting the roles of secondary clays and Fe-oxyhydroxides. Earth Planet Sci. Lett. 243, 760–770.
Seyfferth, A.L., Kocar, B.D., Lee, J.A., Fendorf, S., 2013. Seasonal dynamics of dissolved silicon in a rice cropping system after straw incorporation. Geochim. Cosmichim. Acta 123, 120–133.
Soane, B.D., van Ouwerkerk, C., 1994. Soil compaction problems in world agriculture. In: Soane, B.D., van Ouwerkerk, C. (Eds.), Soil Compaction in Crop Production. Elsevier Science.
Struyf, E., Smis, A., Van Damme, S., Garnier, J., Govers, G., Van Wesemael, B., Conley, D.J., Batelaan, O., Frot, E., Clymans, W., Vandevenne, F., Lancelot, C., Goos, P., Meire, P., 2010. Historical land use change has lowered terrestrial silica mobilization. Nat. Commun. http://dx.doi.org/10.1038/ncomms1128.
Trostle, K.D., Runyon, J.R., Pohlmann, M.A., Redfield, S.E., Pelletier, J., McIntosh, J., Chorover, J., 2016. Colloids and organic matter complexation control trace metal concentration-discharge relationships in Marshall Gulch stream waters. Water Resour. Res. 52, 7931–7944.
Uchida, T., Kosugi, K.N.I., Mizuyama, T., 2001. Effects of pipeflow on hydrological process and its relation to landslide: a review of pipeflow studies in forested headwater catchments. Hydrol. Proced. 15, 2151–2174.
Unzué-Belmonte, D., Ameijeiras-Mariño, Y., Opfergelt, S., Cornélis, J.-T., Barão, L., Minella, J.P.G., Meire, P., Struyf, E., 2017. Land use change affects biogenic silica pool distribution in a subtropical soil toposequence. Solid Earth 8, 737–750.
Wels, C., Cornett, R.J., Lazerte, B.D., 1991. Hydrograph separation: a comparison of geochemical and isotopic tracers. J. Hydrol. 122, 253–274.
Zapata-Rios, X., McIntosh, J., Rademacher, L., Troch, P.A., Brooks, P.D., Rasmussen, C., Chorover, J., 2015. Climatic and landscape controls on water transit times and silicate mineral weathering in the critical zone. Water Resour. Res. 51, 6036–6051.